

Bridge afflux in compound channels

Galip Seçkin, Mehmet Ardiçlıoğlu, Mustafa Mamak* & Serter Atabay
 Civil Engineering Department, Cukurova University, 01330 Adana, Turkey

Received 23 April 2003; accepted 18 August 2003

The results of model testing of arch and straight deck bridge constrictions are presented. All tests were carried out in a compound flume that consists of a main channel and two symmetric floodplains set at a fixed bed slope. A simple generalized afflux equation is also proposed. The equation which describes the model characterizes the afflux as a function of Froude number, and blockage ratio in terms of the downstream conditions.

Bridges cause significant constriction of floodplains during flood events because of their structural design. Thus, they cause increasing upstream flow depth and resulting structural damage to themselves and nature. Hence, one of the most important tasks of a river engineer is to predict the afflux due to bridge structures. Although many investigations of hydraulic behaviour of well-designed straight deck bridges are available¹⁻⁴, there is a little information for arch bridges⁵⁻⁹.

As shown in Fig. 1, the increase (dh) in water surface from the normal stage to the afflux stage at section 1 is known as the afflux of the constriction^{10,11}. The flow through bridge constriction is classified as low flow if it doesn't come into contact with the lower chord of the bridge^{12,13}. When the water surface through the bridge is completely subcritical and profile passes above critical depth, type A low flow occurs. For either subcritical or supercritical profiles, type B flow can exist when the profile passes through critical depth^{12,13}.

Bridge afflux analysis is generally based on the application of either the momentum or the energy principle. When the energy conservation principle is applied to sections 1 and 3 (Fig. 1) for a rectangular channel, afflux value ($dh = h_1 - h_3$) is obtained as follows:

$$dh = \frac{U_3^2 - U_1^2}{2g} + \Delta E \quad \dots (1)$$

where dh is the afflux, U_1 and U_3 are cross-section mean velocities at sections 1 and 3, respectively, g is

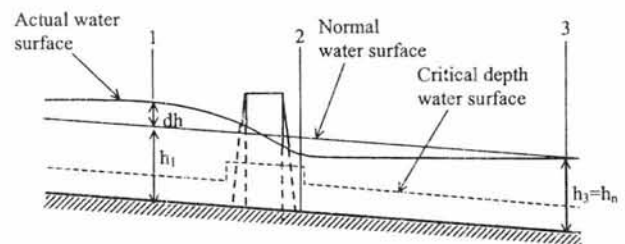


Fig. 1—Definition sketch of flow profiles through a bridge constriction

gravitational acceleration, and ΔE is total energy losses.

Energy losses, through a bridge constriction, include friction, form losses, and eddy losses due to expansion and contractions. In addition, in the case of flood flows, there will be additional losses caused by turbulence and acceleration¹⁴.

Most of the well-known bridge afflux formulae available was developed based on the energy principle^{12,15,16}.

Alternatively, if the momentum conservation principle is applied to sections 1 and 3, afflux value is then obtained as follows⁶:

$$dh = \frac{(Fr_3^2 - 1) + \left[(Fr_3^2 - 1)^2 + 3C_D J_1 Fr_3^2 \right]^{1/2}}{3} \times h_3 \quad \dots (2)$$

where Fr_3 is Froude number at section 3 which refers to normal depth, J_1 is blockage ratio at section 1 (area of bridge below water level/total flow area), and h_3 is normal depth of flow at section 3 ($=h_n$). Here, it should be pointed out that section 3 is located sufficiently downstream from the structure so that the

*For correspondence (E-mail: mmamak@cukurova.edu.tr)

flow is not affected by the bridge (i.e., the flow has fully expanded, and becomes uniform)^{12,13,17}.

For a simple channel of prismatic section where the flow velocity distribution is well-represented by the mean velocity, the Froude number *Fr* is defined by

$$Fr = \sqrt{\frac{Q^2 T}{g A^3}} \quad \dots (3)$$

For a compound channel, the Froude number *Fr* is defined as follows:

$$Fr = \sqrt{\frac{\alpha Q^2 T}{g A^3}} \quad \dots (4)$$

in which α is the kinetic energy flux correction factor which is constant with depth.

Blalock and Sturm^{18,19} showed that both Eqs (3) and (4) produced poor results, and have found that the value of α is not a constant value. Blalock and Sturm^{18,19} also proved that the value of α varies as a function of flow depth in compound channels.

While many methods¹⁸⁻²⁵ are available for predicting critical depth in a compound channel, Lee *et al.*²⁵ noted that the Chaudhry and Bhallamudi²² and Blalock and Sturm¹⁸ approaches have been the most widely used, and the latter is implemented numerically in computer programs such as HEC-RAS¹³. Sturm and Sadiq²⁴ and Lee *et al.*²⁵ pointed out that there is very little difference between the two approaches. In current study, Blalock and Sturm¹⁸ formulae was used for computing the values of Froude number, and given by,

$$Fr = \frac{Q^2}{2g K_T^3} \left(\frac{\sigma_2 \sigma_1}{K_T} - \sigma_1 \right)^{1/2} \quad \dots (5)$$

in which σ_n is the *n*th subsection property defined by Blalock and Sturm¹⁸ as,

$$\sigma_1 = \sum_{i=1}^3 \left[\left(\frac{K_i}{A_i} \right)^3 \left(3T_i - 2R_i \frac{dP_i}{dy} \right) \right] \quad \dots (5a)$$

$$\sigma_2 = \sum_{i=1}^3 \frac{K_i^3}{A_i^2} \quad \dots (5b)$$

$$\sigma_3 = \sum_{i=1}^3 \left[\left(\frac{K_i}{A_i} \right) \left(5T_i - 2R_i \frac{dP_i}{dy} \right) \right] \quad \dots (5c)$$

where A_i is the cross-sectional area and T_i is the top width of flow.

Brown⁶⁻⁸ developed HR Arch Bridge Method based on laboratory experiments conducted at HR Wallingford¹⁷ using Eq. (2) to obtain afflux at arch bridge sites. All the experiments at HR Wallingford were carried out in rectangular flume. HR Method was then verified using the field data collected at arch bridge sites by Regional Water Authorities in UK. All the archived data and records of this major field and laboratory study were re-analyzed at the University of Birmingham^{26,27}. Brown⁷ and Knight and Samuels²⁷ concluded that where the floodplain was poorly defined, some errors occurred at high overbank flows.

Brown⁶⁻⁸ and Hamill & McNally⁹ pointed out that there were not enough reliable field data available for arch bridges. Thus, laboratory experiments retain these popularity to analyze afflux effects through bridge waterways. Nevertheless, most of the laboratory experiments up till recently were carried out to investigate afflux effects in channels with fairly smooth surfaces and having no floodplains^{5,8,28}. In the current study, all the experiments were performed in a compound channel with different roughness patterns²⁹.

Brown⁷ pointed out that present day formulae¹² on bridge hydraulics are appropriate to apply to modern designs of bridges, but are inapplicable to ancient arch structures.

Because of reasons mentioned above, this study is focused on investigation of the hydraulic performance of both single opening and multiple opening arch and straight deck bridge models, which operated under low flow conditions in a compound channel. An attempt is also made to develop a simple afflux formulae that is applicable to both arch and straight deck bridges.

Experimental Procedure

The majority of the tests reported here were performed in a compound channel that consists of a main channel and two symmetric floodplains (Fig. 2) with an 18 m test length at the Hydraulic Laboratory of Birmingham University. The floodplains sides of the flume were constructed of glass materials. The channel bottom was also made of smooth PVC

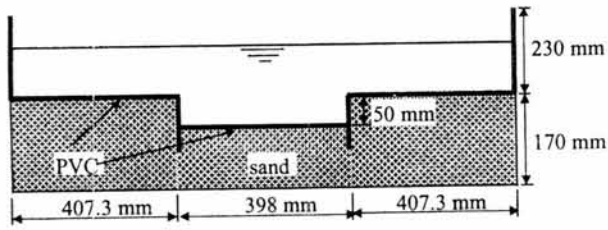
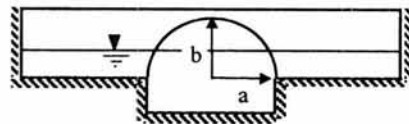
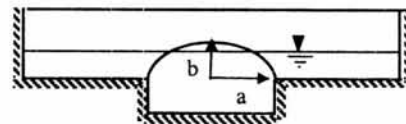


Fig. 2—Cross-section of compound channel flume at Hydraulic Laboratory of Birmingham University

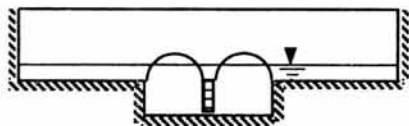
materials. The slope of the flume was fixed at 2.024×10^{-3} . Four bridge models, namely single opening semi-circular arch bridge model (ASOSC), multiple opening semi-circular arch bridge model (AMOSC), single opening elliptical arch bridge model (ASOE), and single opening straight deck bridge model with and without piers (DECK) (Fig. 3a-i), were tested with both smooth and roughened surfaces. The flume has a recirculation system. Discharges were measured



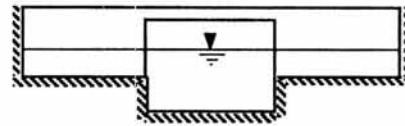
a) Single opening semi-circular arch bridge model (a=19.9 cm, b=19.9 cm)



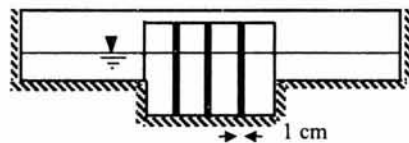
b) Single opening elliptical arch bridge model (a=19.9 cm, b=12 cm)



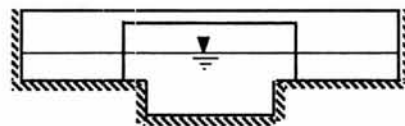
c) Multiple opening semi-circular arch bridge model (a=9.5 cm, b=9.5 cm)



d) Single opening straight deck bridge model without piers (Bridge span width = 0.398m)



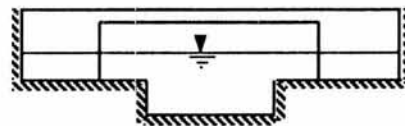
e) Single opening straight deck bridge model with piers (Bridge span width = 0.398m)



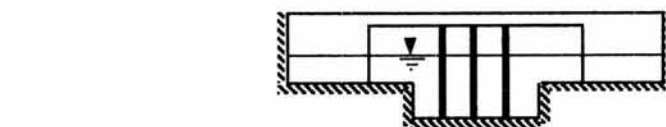
f) Single opening straight deck bridge model without piers (Bridge span width = 0.498m)



g) Single opening straight deck bridge model with piers (Bridge span width = 0.498m)



h) Single opening straight deck bridge model without piers (Bridge span width = 0.598m)



i) Single opening straight deck bridge model with piers (Bridge span width = 0.598m)

Fig. 3—Different types of bridge models used in this study

by an electro-magnetic flow meter, a venturimeter and a dall tube respectively. For the preliminary experiments, at the downstream end of the flume three adjustable tailgates were used to achieve uniform flow conditions when no bridge model existed on the flume. These control gates were adjusted to obtain several M1 and M2 profiles until the water surface slope was equal to the bed slope. Under this condition the average flow depth, known as the normal depth, the average flow velocity was constant for all cross-sections.

Velocity measurements

For each test case, longitudinal direction velocity measurements were all made at the same depth, which was at 0.4 *H* (where *H* is the total depth of flow) from the bed of main flume, using a Novar Nixon miniature propeller current meter with a propeller diameter of 12 mm. Velocity measurements were made by taking five readings at ten second intervals for each 2 cm lateral distance for each test case (Fig. 4).

The section mean velocity (\hat{u}) obtained by integration of the individual local velocity readings (*u*) was compared with the section mean velocity (*U*) obtained from the venturimeter, electro-magnetic flow meter, and dall tube. The mean error between \hat{u} and *U* was 1.21% with a standard deviation of 1.56%.

Roughness conditions

The United States Geological Survey³⁰ reported that floodplain Manning *n* roughness coefficient may increase up to 1.6 for the dense vegetation that is present in many rivers. Chow¹⁰ also pointed out that there may also be some perturbations such as roots, bushes, large logs and other drift on the main channel bottom; trees continually falling into channel because of bank caving. In the laboratory experiments, up till

recently, roughness material used has not reflected these dense vegetation yielding resistances appreciably greater than those of the laboratory inbanks and overbanks.

For reasons explained above, many scenarios were produced, and roughened surfaces were then created by means of various arrangements of aluminium mesh on both floodplains and main channel smooth surfaces together. At the end of these arrangements, roughness coefficient was varied between 0.01 and 0.136 for overbanks, while it ranged from 0.01 to 0.039 for main channel. For representing vegetation, the same roughness elements made of aluminium mesh, were also used by Sellin *et al.*³¹, but these had different dimensions in length, width and height.

Manning roughness coefficients were directly computed using the velocity measurements for main channel and floodplain flow proportions for each case.

Model tests

As shown in Figs 3a-i, nine models were used in the testing program under different boundary roughness conditions. Fifty tests for elliptic and single and multiple semi-circular arch bridge models, and ninety-five tests for straight deck bridge models with and without piers were run for a range of discharges from 0.015 m³/s to 0.055 m³/s. For all tests, each bridge model was placed 8 m downstream from the beginning of the test section. The width of each bridge model was limited to 10 cm with vertical wall abutments.

Water surface profile measurements were made along the centre line of the flume at each location as seen in Fig. 5 for each particular discharge. In this figure, *Q*, *y_n*, *n_{mc}*, and *n_{fp}* demonstrate the discharge, normal depth of flow, main channel Manning

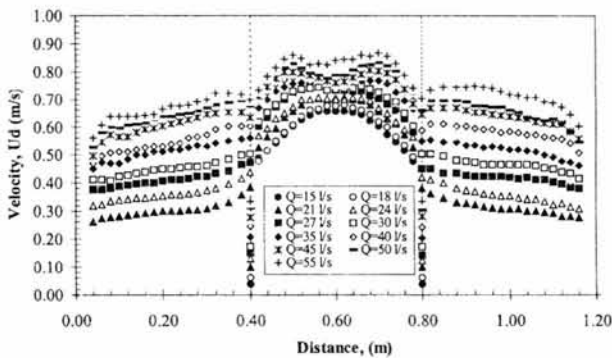


Fig. 4—Comparison of the lateral velocity distribution for the rigid symmetric compound channel for the smooth case.

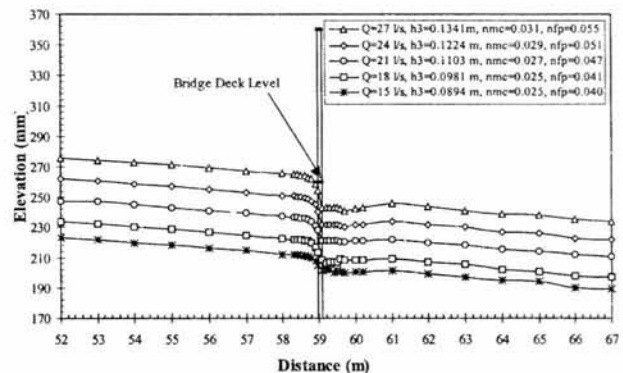


Fig. 5—Measured water surface profiles along the flume

roughness coefficient, and floodplain Manning roughness coefficient, respectively. Normal water surface measurements were made at the same locations (without of bridge models) on the flume for all cases. In the experiments, type A low flow was observed for 100 experimental runs, whereas type B low flow occurred in 45 runs. Types of flow for each test case were also verified using the HEC-RAS package program¹³. The experimental results are given in detail by Seckin²⁹.

Results and Discussion

Eq. (2) demonstrates that dh depends on the downstream Froude number (Fr_3), the upstream blockage ratio (J_1), and drag coefficient (C_D).

Brown⁶ showed that downstream blockage ratio (J_3) may be used instead of J_1 rearranging Eq. (2). Knight and Samuels²⁷ also indicated that Eq. (2) may be developed further using J_3 in place of J_1 , in order to estimate the afflux in terms of the downstream conditions. In current study, these parameters were experimentally obtained. The values of Froude number were computed using Blalock and Sturm formulae¹⁸. Froude number (Fr_3) varied between 0.24 and 1.1, the downstream blockage ratio (J_3) ranged between 0.25 and 0.63. Non-dimensionalized afflux (dh/h_3) values ranged from 0.02 to 0.9 for all test cases. All the experimental work was carried out under low flow conditions.

All measured afflux/normal depth values (dh/h_3) versus Froude number times blockage ratio ($Fr \times J_3$)

are shown in Figs 6-9. Results of square analysis applied to each bridge model, namely single opening semi-circular arch bridge model (ASOSC), multiple opening semi-circular arch bridge model (AMOSC), single opening elliptic arch bridge model (ASOE), and straight deck bridge models with or without piers (DECK) are also given in Table 1. Least square analysis results show that second order polynomial functions are well correlated with the experimental data for each type of bridge model. Experimental results obtained from different types of bridge models including arch and rectangular openings show similar trends with minor differences as can be seen in Figs 6-9. This shows that there is little difference between the behaviour of single rectangular and arched openings. This confirms the earlier findings of Biery and Delleur⁵ and Hamill and McNally⁹.

As shown in Table 1, although each second order polynomial function for each type of bridge models is reasonable for each set of data, a general formulae is proposed to obtain a general equation to give afflux magnitudes for all types of the bridge models used in current study. A meaningful regression is determined as follows, and shown in Fig. 10:

$$\frac{dh}{h_3} = 5.6638 (Fr_3 * J_3)^2 - 1.4445 (Fr_3 * J_3) + 0.1352 \dots (6)$$

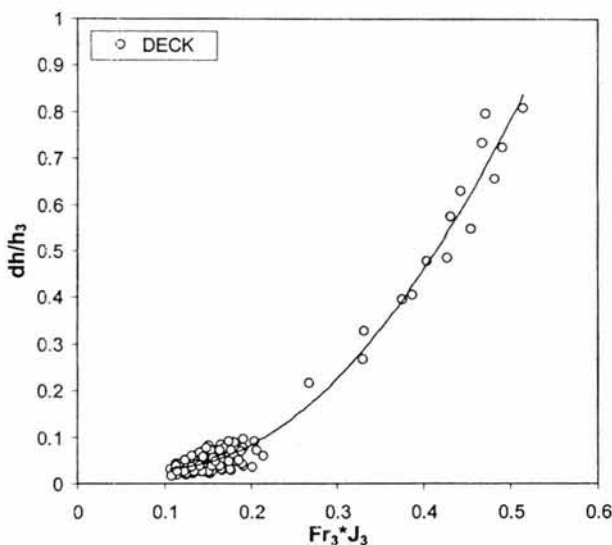


Fig. 6—Plot of dh/h_3 versus $Fr_3 * J_3$ for straight deck bridge models

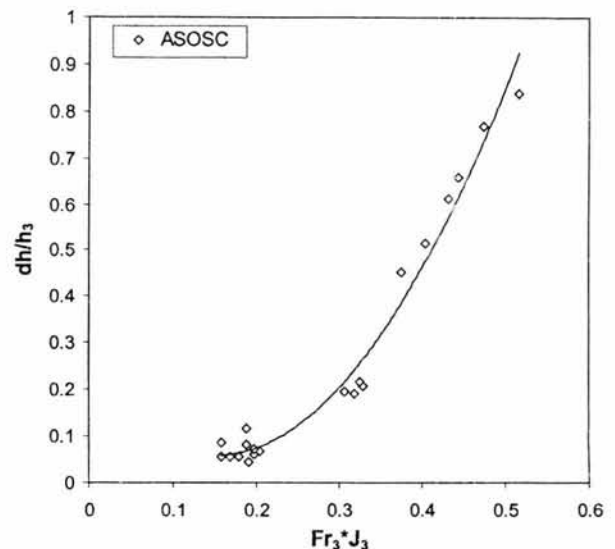


Fig. 7—Plot of dh/h_3 versus $Fr_3 * J_3$ for single opening semi-circular arch bridge model

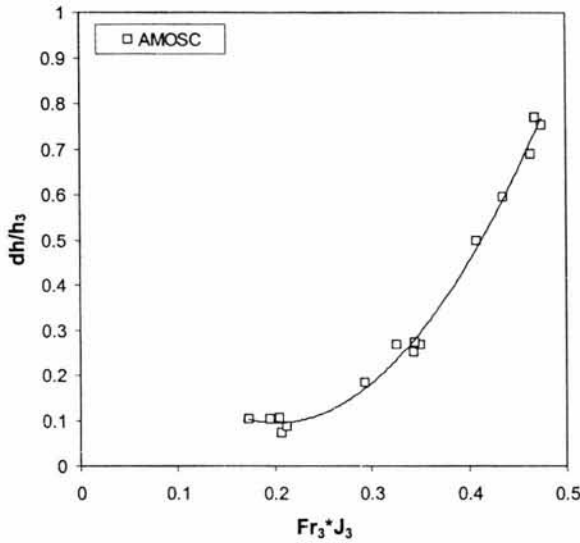


Fig. 8—Plot of dh/h_3 versus Fr_3*J_3 for multiple opening semi-circular arch bridge model

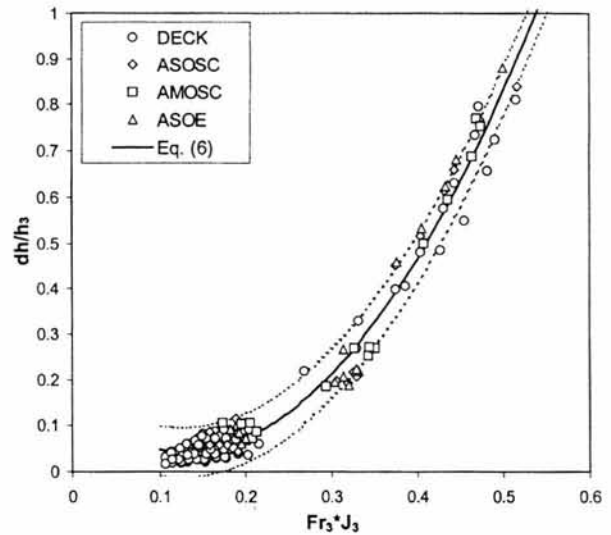


Fig. 10—Plot of dh/h_3 versus Fr_3*J_3 for all types of bridge models used in current study

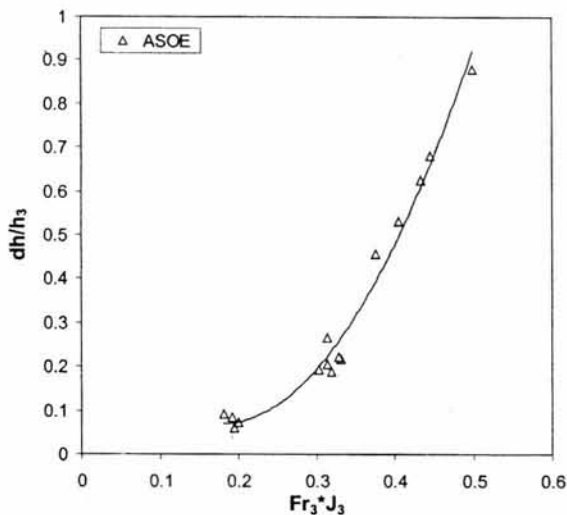


Fig. 9—Plot of dh/h_3 versus Fr_3*J_3 for single opening elliptic arch bridge model

Determination coefficient (R^2) is equal to 0.9796 with a standard deviation of 2.16%. The upper and lower bands in Fig. 10 are 90% confidence level of the relationship established. Using Eq. (6), the prediction interval for afflux in terms of flow depth, with 90% confidence limits, was found to vary in the range of +0.061 to +7.02% on the upper interval and in the range of -6.43 to -0.05% on the lower interval, from low to high values of Froude number and blockage ratio.

Eq. (6) needs to be refined with more experimental data together field data.

Table 1—Least square analysis results applied to each type of bridge model used in current study

Type of bridge	Determination coefficient (R^2)	Experimental dh/h_3 versus $Fr*J_3$ relationships
ASOSC	0.9779	$dh/h_3 = 6.4754 (Fr_3*J_3)^2 - 1.9463 (Fr_3*J_3) + 0.2045$
AMOSC	0.9938	$dh/h_3 = 9.0323 (Fr_3*J_3)^2 - 3.6389 (Fr_3*J_3) + 0.4606$
ASOE	0.9821	$dh/h_3 = 8.2197 (Fr_3*J_3)^2 - 2.921(Fr_3*J_3) + 0.3294$
DECK	0.9807	$dh/h_3 = 4.5229 (Fr_3*J_3)^2 - 0.8333 (Fr_3*J_3) + 0.069$

Although many popular methods which are able to give highly accurate results¹ for afflux are available, the proposed equation (Eq. 6) allows rapid computation of afflux at arch and straight deck bridge sites.

The data presented herein was obtained under the following conditions: $0.4 \times 10^5 < Re < 1.1 \times 10^5$; $0.24 < Fr < 1.1$; $0.22 < U < 0.65$; $15 < Q < 55$.

Conclusions

An empirical equation based on laboratory experiments is established to give afflux at arch and straight deck bridge sites for low flow conditions in compound channels. The equation can predict afflux value with the known values of downstream Froude number, normal depth, and downstream blockage ratio (J_3) of flow with a determination coefficient of 97.96%. This model can be used in the design stage

where very accurate results are not required. Proposed model is limited to type A and type B low flow only in a compound flume with vertical wall abutments.

Acknowledgement

The authors would like to gratefully thank Prof. D W Knight for providing the experimental facilities at Birmingham University Hydraulic Laboratory.

Nomenclature

A	= the cross-sectional area of flow
C_D	= drag coefficient
dh	= afflux
F_r	= Froude number
g	= gravitational acceleration
h	= normal depth of flow
J	= blockage ratio (area of bridge below water level/total flow area)
K_i	= the conveyance of the i th subsection
n_{fp}	= floodplain Manning roughness coefficient
n_{mc}	= main channel Manning roughness coefficient
P_i	= the wetted perimeter for the i th subsection
Q	= discharge
Re	= Reynolds number
R_i	= the hydraulic radius of the cross-section
T	= the top width of water surface
u	= individual local velocity reading
U	= cross-section mean velocity
\hat{U}	= the section mean velocity
ΔE	= total energy losses
α	= kinetic energy flux correction factor
σ_n	= the n th subsection property

References

- Kaatz K J & James W P, *J Hydr Eng, ASCE*, 123 (9) (1997) 784-792.
- Seckin G, Yurtal R & Haktanir T, *J Hydr Eng, ASCE*, 124 (5)(1998) 546-549.
- Biglari B & Sturm T W, *J Hydr Eng, ASCE*, 124 & (2)(1998) 156-164.
- Hunt J, Brunner G W & Larock B E, *J Hydr Engr, ASCE*, 125 (9)(1999) 981-983.
- Biery P F & Delleur J W, *J Hydr Div, Proc ASCE*, 88 (HY2)(1962) 75-108.
- Brown P M, *Hydraulics of bridge waterways: Interim Report*, Report SR 60, HR Wallingford, UK, 1985.
- Brown P M, *Afflux at arch bridges: Second interim report*, Report SR 115, HR Wallingford, UK, 1987.
- Brown P M, *Afflux at arch bridges*, Report SR 182, HR Wallingford, UK, 1988.
- Hamill L & McInally G A, *Inst Civil Eng*, 7 (5) (1990) 241-256.
- Chow V T, *Open-channel hydraulics* {McGraw-Hill, New York}, 1959.
- French R H, *Open-channel hydraulics* {McGraw-Hill, Singapore}, 1987.
- Bradley J N, *Hydraulics of bridge waterways: Hydraulic design. Series no. 1. 2nd Ed.*, Office of Engrg., U.S. Dept. of Transp., Federal Highway Administration, Washington, D. C., 1978.
- HEC-RAS, *River analysis system*, Version 3.1 Beta, Hydrologic Engrg. Ctr., U.S. Army Corps of Engineers, Davis, Calif., 2002.
- Knight A C E, *J Hydr Eng, ASCE*, 114 (7) (1988) 757-766.
- Kindsvatner C E, Carter R W & Tracy H J, *Computation of peak discharge at contractions*, U. S. Geological Survey Circular 284, Washington, D. C., 1953.
- Shearman J O, *User's manual for WSPRO, a computer model for water surface profile computation*, Rep. No. FHWA-IP-89-027, U.S. Geological Survey, Reston, Va., 1990.
- ISIS, *ISIS Flow user manuel*, Sir William Hallcrow & Partners and HR Wallingford, Version 2.1, England, 2002.
- Blalock M E & Sturm T W, *J Hydr Div, ASCE*, 107 (1981) 699-717.
- Blalock M E & Sturm T W, *J Hydr Div, ASCE*, 109 (1983) 483-486.
- Petryk S & Grant E U, *J Hydr Div, ASCE*, 104 (HY5) (1978) 583-594.
- Schoellhamer D H, Peters J C & Larock B E, *J Hydr Eng, ASCE*, 111 (7) (1985) 1099-1104.
- Chaudhry M H & Bhallamudi S M, *J Hydr Res*, 26 (4)(1988) 377-396.
- Yuen K W H & Knight D W, *Critical flow in two stage channel*, Proc. Int. Conf. River Flood Hydraulics, 17-20 September 1990.
- Sturm T W & Sadiq A, *J Hydr Eng, ASCE*, 122 (12)(1996) 703-709.
- Lee P J, Lambert M F & Simpson A R, *Critical depth prediction in straight compound channels*, Proc. Inst Civil Eng, Water & Maritime Engineering, 154 (4)(2002)317-332.
- Sheikh A P, *Critical analysis of bridge afflux formulae*, Industrial Project Report for HR Wallingford, as part fulfilment of MSc (Eng) degree, Water Resources Technology and Management Course, The University of Birmingham, 1-150, 1997.
- Knight, D W & Samuels P G, *Localised flow modelling of bridges, sluices and hydraulic structures under flood flow conditions*, Proc. 34th MAFF Conf of River and Coastal Engineers, Keele University, June, [C], (1999), pp 1.2.1-1.2.13.
- Charbeneau R J & Holley E R, *Backwater effects of bridge piers in subcritical flow*, Research Report, No:0-1805-1, Texas Dept. of Transportation in cooperation with the U.S. Dept. of Transportation, FHWA, 1-102, 2001.
- Seckin G, *Theoretical and experimental analysis of backwater due to different types of bridge structures on rivers*, Ph D Thesis, The University of Cukurova, Turkey, 2001.(In Turkish).
- United States Geological Survey (USGS), *Guide for selecting Manning's roughness coefficients for natural channels and flood plains*, Water-Supply Paper 2339, Reston, Va., 1989.
- Sellin R H J, Bryant T B & Loveless J H, *J Hydr Res, IAHR*, 41 (1)(2003) 3-14.